INL/CON-23-71453-Revision-0

Uncertainty-aware photovoltaic generation estimation through fusion of physics with harmonics information using Bayesian neural networks

January 2023

Changing the World's Energy Future

Dimitrios Stylianos Parsinas Pylorof, Humberto Enrique Garcia

Idaho National Laboratory

INL/CON-23-71453-Revision-0

Uncertainty-aware photovoltaic generation estimation through fusion of physics with harmonics information using Bayesian neural networks

Dimitrios Stylianos Parsinas Pylorof, Humberto Enrique Garcia

January 2023

Idaho National Laboratory
Idaho Falls, Idaho 83415

http://www.inl.gov

Prepared for the
U.S. Department of Energy
Under DOE Idaho Operations Office
Contract DE-AC07-05ID14517

Uncertainty-aware photovoltaic generation estimation through fusion of physics with harmonics information using Bayesian neural networks

Dimitrios Pylorof Humberto E. Garcia

Abstract—**We develop an aggregate photovoltaic generation estimation methodology that uses diverse inputs and can reason on its current input-dependent predictive uncertainty. Named PV-PHEst, for PhotoVoltaic Physics- & Harmonics-driven Estimator, the resulting tool is intelligently weighing and fusing information carried by the output of physics models, harmonics, and line sensors, using Bayesian neural networks and related techniques aimed at solving machine learning problems with intrinsic uncertainty quantification. As each of the three input classes carries heterogeneous information that only sheds light on one facet of the estimation problem but its value can diminish in the face of diverse grid phenomena, PV-PHEst with its estimation and uncertainty reasoning capabilities perform a nontrivial and potentially mission-critical task of value to grid operators.**

Index Terms—**Photovoltaic systems, Analytics, Machine learning, Uncertainty quantification, Bayesian methods**

I. Introduction

Massively distributed energy generation within distribution grids, as typically achieved nowadays using solar photovoltaic distributed energy resources (PV-DERs), is key to achieving energy resiliency and self-sufficiency at the community level, as well as to reaching pressing renewable energy penetration objectives. Nevertheless, solar energy generation tends to be volatile, and the distributed structure of solar-heavy grids complicates significantly the task of managing power flows and ensuring stable grid operation, often by controlling additional, possibly non-solar energy resources. To perform such mission-critical control, grid operators need visibility on real-time solar generation of their grids. As over-instrumenting the grid with DER- (and customer-)specific sensors is often unfeasible due to cost, communication burden, and privacy reasons, solar generation needs to be estimated and predicted with whatever information sources may be available, and algorithmic techniques addressing the so-called *solar disaggregation* problem.

Assuming, unrealistically, perfect information about an area's PV infrastructure (including panel geometry and other equipment characteristics for *all* distributed installations), real-time environment sensing, and physics models of adequate fidelity leads to a trivial yet infeasible solution to the problem, where PV generation is analytically calculated for each and every prosumer in the focus area. Conversely, assuming significant real-time grid instrumentation (to include all consumption and centralized generation of electricity) leads to another analytically trivial but practically infeasible solution to the problem, where one balances power flows using information from all centralized power plants and/or substations, prosumers, and consumers of electricity. In between the aforedescribed extreme scenarios, the technical community has been devoting significant efforts to solve the solar disaggregation problem under various permutations of sensing, analytical, and statistical tools. We indicatively refer to [1], where a game-theoretic approach is used in solar disaggregation by including fully-instrumented prosumers in the mix and reasoning on their correlations with non-instrumented prosumers, to [2], where a utility-in-the-loop approach offers greater attention to the issues of privacy and distributed learning, to [3], where PV and non-PV customers are statistically correlated via their diurnal-nocturnal loads to the end of inferring PV-equipped prosumer behavior, to the more statistical, unsupervised approach of [4], and ultimately, to the more data-driven approach of [5] with particular focus on prosumer heterogeneity.

In this paper, we develop PV-PHEst (PhotoVoltaic Physics- & Harmonics-driven Estimator), a novel PV generation estimation capability capable to reason on the uncertainty of its output, and to fuse and enhance the value of judiciously selected yet disparate information sources. PV-PHEst is using multi-modal input consisting of: (a) uncertain, model-based information, as those that would be available for a massively distributed grid of heterogeneous prosumers (whose installation parameters cannot be perfectly determined and maintained) and (b) line sensor measurements and their harmonic decomposition. Harmonic distortion carries information relatable to PV generation, but it can be contaminated by the dynamic operation of other harmonics-inducing sources. Models carry invaluable, albeit inaccurate information. PV-PHEst performs its fusion task by means of training and then using operationally a machine learning regressor based on Bayesian neural networks. As shown via numerical evaluations, PV-PHEst is able to amplify the value of either information source, producing disaggregation outputs with quantified uncertainty of use to grid stakeholders, even under significant uncertainty and grid disturbances.

D. Pylorof and H. E. Garcia are with the Systems Science & Engineering Division of the U.S. Department of Energy Idaho National Laboratory, Idaho Falls, ID 83415, USA.
Corresponding author: H. E. Garcia (`humberto.garcia@inl.gov`).

The work presented herein was funded in part by Project PV-NOW of the U.S. Department of Energy Office of Electricity through Contract No. DE-AC07-05ID14517.

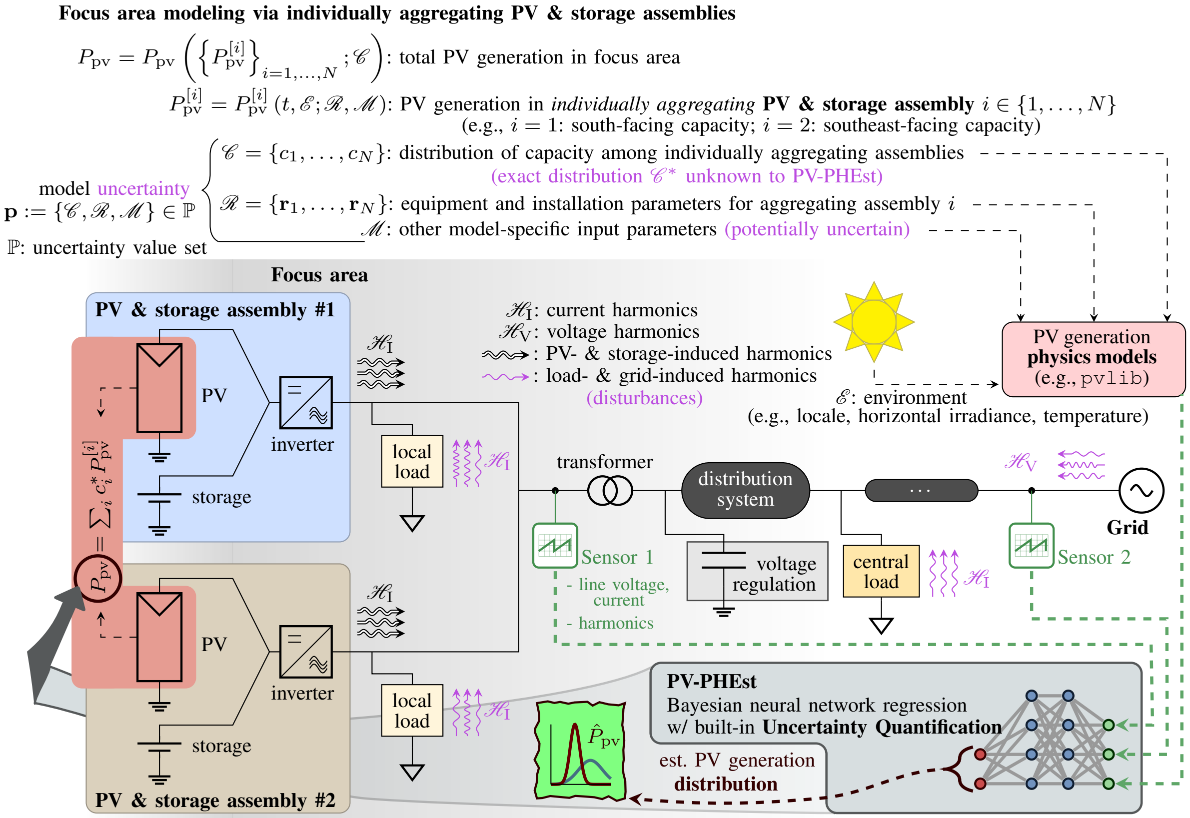

Fig. 1: Electrical and logical architecture for PV-PHEst design, development, evaluation, and deployment.

II. Preliminaries

A. Physics models

Energy conversion processes in photovoltaic equipment, as well as effects of materials, environmental aspects, and other physical and/or chemical phenomena are nowadays well understood and modeled in sufficient fidelity for many applications by inclusive libraries such as `pvlib` [6]. In the modeling paradigm of interest for the present work, `pvlib` is employed for a particular locale and PV installation with specific geometry and capacity data to calculate irradiance-type quantities, cell temperatures given ambient conditions, and, ultimately, PV-produced DC power. Corrections to irradiance quantities for the presence of clouds are implemented according to [7]. It is key to be cognizant of two types of modeling errors, which both contribute to aleatoric uncertainty in the sought-after PV generation estimate: (a) even mature and well-studied models introduce errors; (b) the input conditions to any such models may not correspond to ground truth. To illustrate, it is rather difficult to capture with enough accuracy the geometry and equipment characteristics for PVs in all prosumers across a certain area of interest and to keep such information up-to-date, not to mention location-specific short-fuse phenomena such as shading from trees and degradation from dust; any model's original accuracy will thus decrease. Nevertheless, information from dispatchable (i.e., executable online and potentially embeddable on field hardware) models is still valuable, even under significant modeling uncertainty. PV-PHEst demonstrates the added value when operationally imperfect models are intelligently fused with information-rich signals collected from few line sensors. We denote the potentially uncertain parameters for any physics model describing the PV generation in the focus area by $\mathbf{p} \in \mathbb{P}$, where $\mathbb{P}$ is the compact value set where elements of $\mathbf{p}$ are assumed to be constrained, assuming deterministically bounded uncertainty. Without significant changes, one could alternatively consider a more general stochastic case for $\mathbf{p}$.

B. Harmonics generation and contamination

DC sources, as are PV solar panels and batteries, are typically connected to the AC part of the grid via an inverter. Due to their operating principles, inverters produce *imperfect* sine waves containing additional frequencies other than the fundamental and resulting in the phenomenon of *harmonic distortion* [8]. Inductive and capacitive loads as well as other elements across the grid also cause harmonic distortion, albeit possibly at different levels of power per frequency compared to inverters. To promote grid stability, various standards impose bounds on both power at individual frequencies and the *total harmonic distortion*, per single grid element, as well as for the grid at large [9], [10]. Even if harmonic distortion is generally considered to be a stability-threatening nuisance for the grid, it is an inevitable phenomenon, which, in the case of harmonic distortion caused by PV-related inverters, can carry -nonetheless- useful information on the amount of DC power an inverter is converting to AC, since distortion levels on particular frequencies for varying inverter output follow algorithmically identifiable patterns, evidenced in Section V. In view of our disaggregation objective and the use of information-carrying harmonics by PV-PHEst, we refer to non-PV-related (e.g., induced by loads or the grid) harmonics as *contaminants* acting as a disturbance to our PV power estimation objective, alongside modeling uncertainty.

C. UQ-equipped regression with Bayesian neural networks

Machine learning regression is a staple in supervised statistical learning, where a model is constructed from a dataset, containing input/output pairs, to be able to predict outputs from (potentially unseen before) inputs drawn from the same distribution where the dataset originated. Regression models can be constructed using numerous traditional and emerging techniques, ranging from least squares to kernel methods, Gaussian processes, to various approaches based on neural networks. Regardless of the discriminatory capabilities of the model and any other traits of interest (e.g., generalization, computational efficiency, robustness), any regressor in realistic circumstances will exhibit uncertainty, which can be broadly understood as: (a) *model (or epistemic) uncertainty*, related to the regressor's (in)ability to approximate knowledge encapsulated in the dataset (e.g., where the regressor's structure cannot fit to the sought-after mapping), and (b) *data (or aleatoric) uncertainty*, related to ambiguities in the dataset (e.g., where similar inputs seem to lead to dissimilar outputs). In our work and regression task, we employ Bayesian neural networks (BNNs) [11], which fit distributions to their unknowns during training and are designed to produce input-dependent expected values and standard deviations as output to any given input when used operationally as regressors. We refer to `UQ360` [12] and to `TensorFlow Probability` [13] as indicative BNN-inclusive machine learning libraries [14].

III. Aggregate modeling & demo topology

To illustrate the significant uncertainty in PV generation models that can manifest in grids that are neither over-instrumented nor over-documented, we consider an aggregate modeling approach where a particular focus area with 400 kW installed capacity is split evenly into south-facing ($i = 1$) and southeast-facing ($i = 2$) capacity. Even if the (even) distribution is fixed in our high-fidelity simulators (as would be fixed, at least over reasonable amounts of time, also in reality), having operational uncertainty over both the respective distribution $\mathscr{C} = \{c_1, c_2\}$ and the total capacity itself (e.g., $\pm 10 \sim 20\%$) can cause significant errors in the output of models such as `pvlib`, at any given time during the day, and on top of any errors caused by instrumentation noise or other discrepancies between modeled and ground truth (or real-life) physics. On top of the two individually aggregating PV and storage assemblies, the considered topology consists of local loads with time-varying inductive and capacitive (and, thus, harmonics-inducing) components, a distribution system with necessary elements, a central load, again, with inductive/capacitive components, and a connection to the grid. Two line sensors measuring current and voltage, as well as performing a harmonic decomposition are installed close to the individually aggregating PV and storage assemblies and the grid, respectively. It is also assumed that (noisy) environmental measurements are available for the focus area. The demonstration topology, illustrating the aggregate modeling approach, grid elements, and instrumentation, is summarized by Figure 1.

Even if our modeling approach has been motivated by the aforedescribed aspects and particular focus on operational deployment constraints in locales where precise PV installation details may not be easy to obtain and maintain, using individually aggregating PV assemblies with uncertainty in capacities is not binding for the development and deployment of PV-PHEst. It is envisioned that any uncertain physics model (no matter where the uncertainty comes from) can be fused with contaminated harmonics signatures to weigh and amplify the value of information carried by each source.

IV. Solution architecture and workflows

PV-PHEst fits the demonstration topology or any deployment target as illustrated in Figure 1 by receiving inputs from: (a) dispatchable PV physics models (e.g., `pvlib` running with an approximate description of the focus area and environmental measurements), and (b) a limited number of line sensors providing current and voltage measurements and their corresponding harmonic decompositions. The technical objective for PV-PHEst is to understand the relation between ground truths for PV generation (unknown and unseen as PV-PHEst operates) and values of input features that correspond to said ground truths. After capturing such knowledge, PV-PHEst reasons on the likelihood of PV-generation using inputs (a) and (b). An offline training phase is conducted to create applicable datasets and equip PV-PHEst with the required experience, either prior to any deployment or whenever changes to the focus area occur. Afterwards, PV-PHEst is used operationally by providing real-time inputs (a) and (b) to the trained BNN and obtaining an estimated PV generation distribution in terms of the expected value and standard deviation. The respective workflows are illustrated in Figure 2.

V. Numerical evaluation

In the context of the present work, storage was present in the topology but not changing its operational mode (e.g., from charging to discharging). The ground truth model was developed and simulated in MATLAB/Simulink with Simscape Electrical, using physics elements from `pvlib`, with ground truth parameters $\mathbf{p}^* \in \mathbb{P}$ unknown to downstream modules, including PV-PHEst, except for the bounds described $\mathbb{P}$ corresponding to $0.9 \leq c_1 \leq 1.2$ and $0.8 \leq c_2 \leq 1.15$, and zero-mean instrumentation noise up to $\pm 5\%$. Further physics model uncertainty was artificially injected in parts of the operational regime (e.g., low temperatures, low irradiance decrease accuracy of physics model). A variant of the `pvlib` model is used operationally, with parameters $\mathbf{p}' \in \mathbb{P}$ (i.e., within the assumed value set but not equal to ground truth values $\mathbf{p}^*$). Two evaluations are performed, for moderate and significant disturbances, where harmonic distortion from the grid and each load are up to 40% and 100%, respectively, of the levels given in IEEE Std. P519. In each evaluation, a dataset of

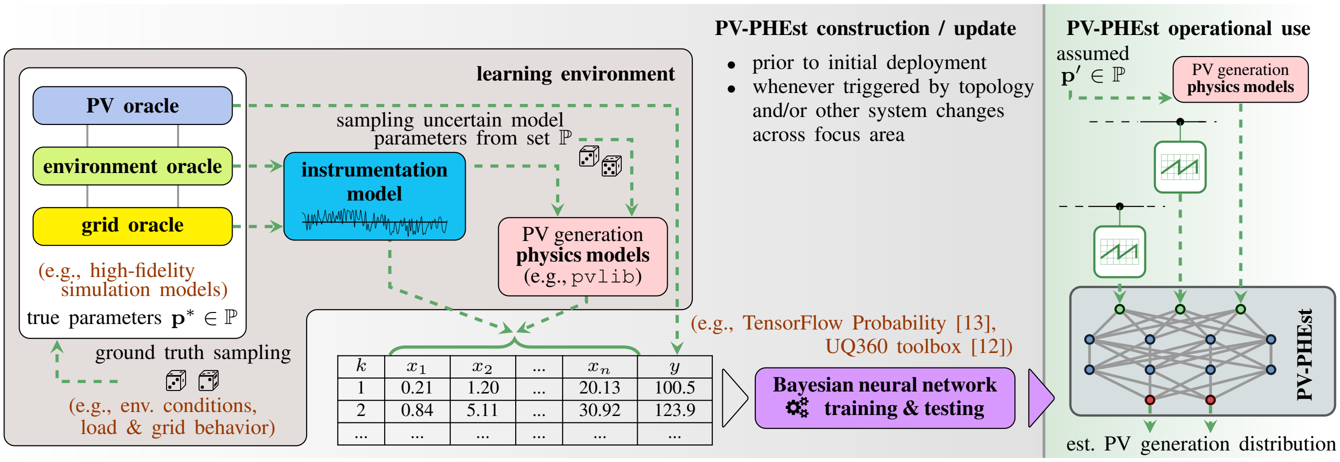

Fig. 2: PV-PHEst workflows. After an offline training phase where PV-PHEst is constructed or updated, the resulting BNN is used operationally.

12,000 cases from the simulated demonstration topology is collected, while creating input features by sampling uniformly from $\mathbb{P}$. This dataset is then randomly split into a training and test set of 8,400 and 3,600 cases, respectively. PH-PHEst is then configured, with a single hidden layer of 20 nodes using `UQ360`, and a BNN with weights following a horseshoe prior distribution, subsequently trained with the `Adam` optimizer using a learning rate of 0.005 for 3,000 epochs and a batch size of 100 samples per update. Validation results on the (unseen during PV-PHEst construction) test set for each of the two evaluations are tabulated in Table I, and illustrated in Figure 3. In each evaluation, we compare error performance on unseen data among **Baseline B1:** a BNN synthesized only with line sensor (incl. harmonics) inputs, i.e., PV-PHEst "without" physics; **Baseline B2:** raw output of physics models; **Baseline B3:** a BNN attempting to adjust physics models across the operational regime, i.e., PV-PHEst "without" line sensors; and **PV-PHEst**. It is evident that regardless of the uncertainty of either information source, the intelligent fusion provided by PV-PHEst offers a more accurate and valuable output, even in the highly-disturbed scenario where **B1** deteriorates significantly (in the presence of more harmonics contaminants) yet the underlying signatures are still useful to PV-PHEst in conjunction with physics model outputs. The distributions of PV-PHEst's understanding of uncertainty throughout the 12,000 case datasets, in terms of BNN-computed standard deviation, are illustrated in Figure 4 for the two evaluations. One can observe that PV-PHEst appears to be self-aware of the higher uncertainty in Evaluation 2. Finally, PV power estimation results with uncertainty quantification, as they would have been provided to a grid operator, are illustrated in Figure 5 for two different inputs.

VI. Conclusion & Future Work

We presented PV-PHEst, a BNN-based approach to the solar disaggregation problem. PV-PHEst can amplify the value of diverse information sources consisting of (limited) line sensors covering a focus area, the corresponding harmonics decompositions, and approximate physics models. Future work will focus on incorporating appropriate load modeling as a

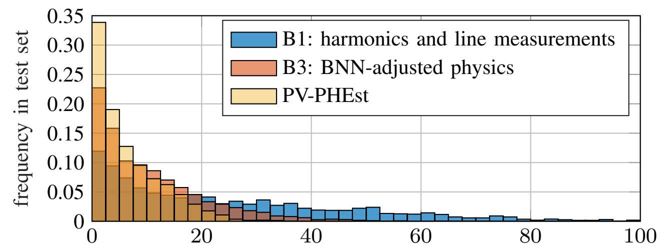

(a) Evaluation 1 - moderate disturbances

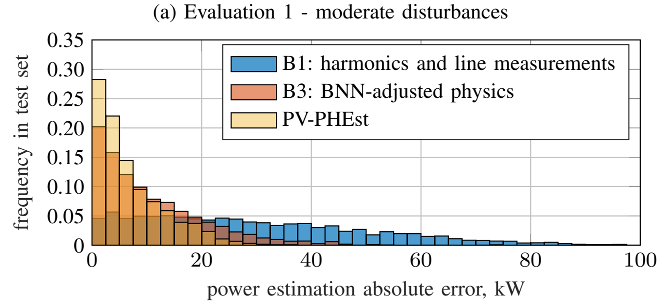

(b) Evaluation 2 - significant disturbances

Fig. 3: Comparative error distribution across test set. PV-PHEst can be seen to amplify the value of information from both its sources, even under significant uncertainty.

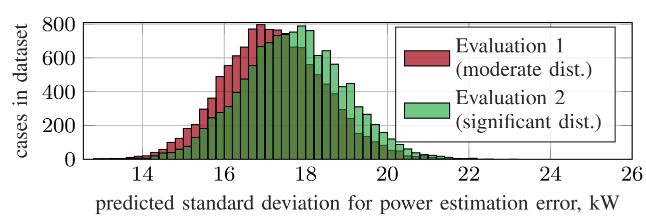

Fig. 4: PV-PHEst's understanding of uncertainty across Evaluations 1 & 2.

third information source modality, and progressive hardware-in-the-loop evaluations with actual line sensors.

Acknowledgment

The authors acknowledge the contributions of Rojan Bhattarai and Temitayo Olowu to relevant model development.

References

[1] F. Bu, K. Dehghanpour, Y. Yuan, Z. Wang, and Y. Zhang, "A data-driven game-theoretic approach for behind-the-meter PV generation

Evaluation 1 - moderate disturbances (up to 40% of levels from IEEE Std. P519)							
	absolute error on test set (unseen during construction of each method)						
	$\leq$ **2.5 kW** ($\leq 0.625\%$ IC)	$\leq$ **5 kW** ($\leq 1.25\%$ IC)	$\leq$ **10 kW** ($\leq 2.5\%$ IC)	$\leq$ **20 kW** ($\leq 5\%$ IC)	$\leq$ **30 kW** ($\leq 7.5\%$ IC)	$\leq$ **40 kW** ($\leq 10\%$ IC)	$>$ **40 kW** ($> 10\%$ IC)
Baseline B1: harmonics & line meas.	430 cases (12% of TS)	770 cases (21% of TS)	1,036 cases (29% of TS)	1,241 cases (34% of TS)	1,414 cases (39% of TS)	1,574 cases (44% of TS)	2,026 cases (56% of TS)
Baseline B2: physics (raw)	648 cases (18% of TS)	693 cases (19% of TS)	740 cases (21% of TS)	777 cases (22% of TS)	806 cases (22% of TS)	852 cases (24% of TS)	2,748 cases (76% of TS)
Baseline B3: ML-adjusted physics	818 cases (23% of TS)	1,388 cases (39% of TS)	1,758 cases (49% of TS)	2,100 cases (58% of TS)	2,410 cases (67% of TS)	2,663 cases (74% of TS)	937 cases (26% of TS)
PV-PHEst	1,219 cases (34% of TS)	1,904 cases (53% of TS)	2,363 cases (66% of TS)	2,709 cases (75% of TS)	2,970 cases (83% of TS)	3,195 cases (89% of TS)	405 cases (11% of TS)
Comparisons per each error interval							
PV-PHEst vs. B1	183% better	147% better	128% better	118% better	110% better	102% better	80% better
PV-PHEst vs. B3	49% better	37% better	34% better	29% better	23% better	20% better	57% better
Evaluation 2 - severe disturbances (up to 100% of levels from IEEE Std. P519)							
	absolute error on test set (unseen during construction of each method)						
	$\leq$ **2.5 kW** ($\leq 0.625\%$ IC)	$\leq$ **5 kW** ($\leq 1.25\%$ IC)	$\leq$ **10 kW** ($\leq 2.5\%$ IC)	$\leq$ **20 kW** ($\leq 5\%$ IC)	$\leq$ **30 kW** ($\leq 7.5\%$ IC)	$\leq$ **40 kW** ($\leq 10\%$ IC)	$>$ **40 kW** ($> 10\%$ IC)
Baseline B1: harmonics & line meas.	166 cases (5% of TS)	370 cases (10% of TS)	535 cases (15% of TS)	714 cases (20% of TS)	891 cases (25% of TS)	1,072 cases (30% of TS)	2528 cases (70% of TS)
Baseline B2: physics (raw)	620 cases (17% of TS)	661 cases (18% of TS)	698 cases (19% of TS)	745 cases (21% of TS)	781 cases (22% of TS)	819 cases (23% of TS)	2781 cases (77% of TS)
Baseline B3: ML-adjusted physics	727 cases (20% of TS)	1,295 cases (36% of TS)	1,728 cases (48% of TS)	2,085 cases (58% of TS)	2,368 cases (66% of TS)	2,631 cases (73% of TS)	969 cases (27% of TS)
PV-PHEst	1,018 cases (28% of TS)	1,811 cases (50% of TS)	2,332 cases (65% of TS)	2,674 cases (75% of TS)	2,941 cases (81% of TS)	3,153 cases (88% of TS)	447 cases (12% of TS)
Comparisons per each error interval							
PV-PHEst vs. B1	513% better	389% better	336% better	275% better	230% better	194% better	82% better
PV-PHEst vs. B3	40% better	40% better	35% better	28% better	24% better	20% better	53% better

TABLE I: Numerical results from Evaluations 1 and 2. IC: installed capacity (400 kW) TS: test set (3,600 cases)

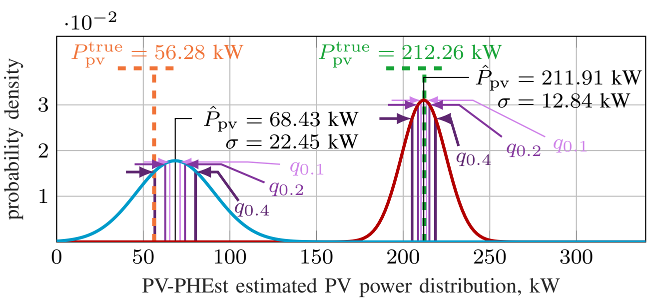

Fig. 5: PV power estimation in terms of fitted normal distributions by PV-PHEst for two distinct example cases. On the left, PV-PHEst is less confident compared to the case on the right, as seen by the difference in estimated standard deviations σ and the corresponding probability density shapes. Using known properties of the normal distribution, we calculate practically useful confidence intervals $q_\rho : \left[\hat{P}_{\mathrm{pv}} - g(\sigma,\rho), \hat{P}_{\mathrm{pv}} + g(\sigma,\rho)\right]$ in which the true value is estimated to lie with probability $\rho \in (0,1)$, where $g(\sigma,\rho) := \sigma\sqrt{2}\mathrm{erf}^{-1}\rho$ and erf^{-1} is the inverse of the error function. For the case on the right, with estimated expected value $\hat{P}_{\mathrm{pv}} = 211.91$ kW, the intervals where the true value is estimated to lie with 10%, 20%, and 40% probability are $q_{0.1} : [210.30, 213.52]$ kW, $q_{0.2} : [208.66, 215.16]$ kW, and $q_{0.4} : [205.18, 218.64]$ kW, respectively, even if the expected value happened to be spot on. For the case on the left where PV-PHEst is less confident, the corresponding intervals are illustrated on the plot.

disaggregation," *IEEE Transactions on Power Systems*, vol. 35, no. 4, pp. 3133–3144, 2020.

[2] J. Lin, J. Ma, and J. Zhu, "A privacy-preserving federated learning method for probabilistic community-level behind-the-meter solar generation disaggregation," *IEEE Transactions on Smart Grid*, vol. 13, no. 1, pp. 268–279, 2021.

[3] F. Bu, K. Dehghanpour, Y. Yuan, Z. Wang, and Y. Guo, "Disaggregating customer-level behind-the-meter PV generation using smart meter data and solar exemplars," *IEEE Transactions on Power Systems*, vol. 36, no. 6, pp. 5417–5427, 2021.

[4] F. Kabir, N. Yu, W. Yao, R. Yang, and Y. Zhang, "Joint estimation of behind-the-meter solar generation in a community," *IEEE Transactions on Sustainable Energy*, vol. 12, no. 1, pp. 682–694, 2020.

[5] F. Sossan, L. Nespoli, V. Medici, and M. Paolone, "Unsupervised disaggregation of photovoltaic production from composite power flow measurements of heterogeneous prosumers," *IEEE Transactions on Industrial Informatics*, vol. 14, no. 9, pp. 3904–3913, 2018.

[6] J. S. Stein, W. F. Holmgren, J. Forbess, and C. W. Hansen, "PVLIB: Open source photovoltaic performance modeling functions for Matlab and Python," in *2016 IEEE 43rd Photovoltaic Specialists Conference*, 2016, pp. 3425–3430.

[7] L. Luo, D. Hamilton, and B. Han, "Estimation of total cloud cover from solar radiation observations at Lake Rotorua, New Zealand," *Solar Energy*, vol. 84, no. 3, pp. 501–506, 2010.

[8] A. Bosman, J. Cobben, J. Myrzik, and W. Kling, "Harmonic modelling of solar inverters and their interaction with the distribution grid," in *Proceedings of the 41st International Universities Power Engineering Conference*, vol. 3. IEEE, 2006, pp. 991–995.

[9] *IEEE Standard for Interconnection and Interoperability of Distributed Energy Resources with Associated Electric Power Systems Interfaces*, IEEE Std. 1547-2018, 2018.

[10] *IEEE Draft Standard for Harmonic Control in Electric Power Systems*, IEEE Std. P519/D5.1, 2021.

[11] S. Ghosh, J. Yao, and F. Doshi-Velez, "Structured variational learning of Bayesian neural networks with horseshoe priors," in *International Conference on Machine Learning*, 2018, pp. 1744–1753.

[12] S. Ghosh, Q. V. Liao, K. N. Ramamurthy, J. Navratil, P. Sattigeri, K. R. Varshney, and Y. Zhang, "Uncertainty Quantification 360: A holistic toolkit for quantifying and communicating the uncertainty of AI," 2021. [Online]. Available: https://arxiv.org/abs/2106.01410

[13] J. V. Dillon, I. Langmore, D. Tran, E. Brevdo, S. Vasudevan, D. Moore, B. Patton, A. Alemi, M. Hoffman, and R. A. Saurous, "TensorFlow distributions," *arXiv preprint arXiv:1711.10604*, 2017.

[14] M. Pintz, J. Sicking, M. Poretschkin, and M. Akila, "A survey on uncertainty toolkits for deep learning," *arXiv preprint arXiv:2205.01040*, 2022.